Studying electroweak sector of the Standard Model with the ATLAS detector

Rustem Ospanov

University of Science and Technology of China

May 10, 2019

Introduction

- SM is a relativistic renormalizable quantum theory of 12 fermions with 3 forces mediated by spin-1 gauge bosons
- $SU(2) \times U(1)$ gauge symmetry is spontaneously broken by the Brout-Englert-Higgs mechanism $\leftrightarrow$ massive $W^{\pm}$ and Z bosons

- All SM parameters are measured experimentally (except for some of neutrino parameters):
  - α_{QCD}
  - fermion masses and mixing
  - m_H, m_Z, G_F, fine structure constant
- SM predictions $\sim$agree with data
- **SM is self-consistent but not complete**

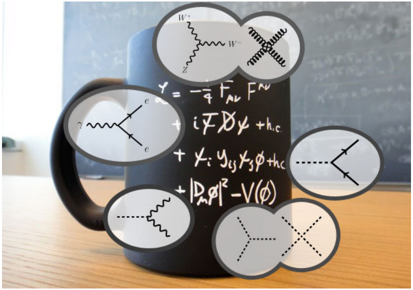

Image by Flip Tanedo

Electroweak properties are determined by $SU(2) \times U(1)$ gauge symmetry

- Test EW predictions at the LHC with di-boson processes

Charged gauge boson self-couplings are present at tree level in SM:

- Triple couplings: WWZ, $WW\gamma$
- Quartic couplings: $WWZZ$, $WWWW$, $WWZ\gamma$, $WW\gamma\gamma$

Neutral gauge boson self-couplings are absent at tree level in SM:

- $ZZ\gamma$, ZZZ, $ZZ\gamma\gamma$, $ZZZZ$...

Outline

Introduction to LHC and ATLAS

Vector Boson Scattering

- Sensitive to gauge boson quartic coupling
- **Results at 13 TeV: electroweak production of WZ and same sign WW**

Di-boson production measurements

- Probe gauge structure of SM with high precision
- Sensitive to gauge boson triple coupling
- **Results at 13 TeV: WZ cross sections**

Z boson differential cross sections

- **Effective leptonic weak mixing angle $\sin\theta^{l}_{\text{eff}}$ with 8 TeV data**

Large Hadron Collider

- 4 input accelerators inject 450 GeV proton beams
- 9593 magnets $\rightarrow$ 1232 superconducting dipoles
- 8 RF cavities accelerate protons up to 6.5 TeV
- \$3.6 billion USD construction costs
- \$1.1 billion USD operational costs for 2009-2012
- 3 quadrupole magnets focus beams at collision points
- Transverse proton beam size in:
  - the bending dipoles: $\sim$ 0.2 mm
  - the focusing magnets: $\sim$ 1.6 mm
  - ATLAS and CMS: $\sim$ 0.016 mm

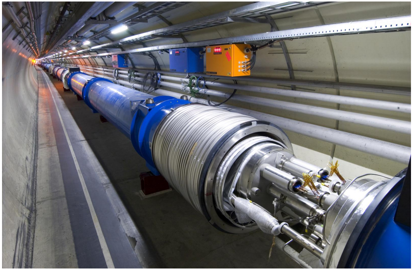

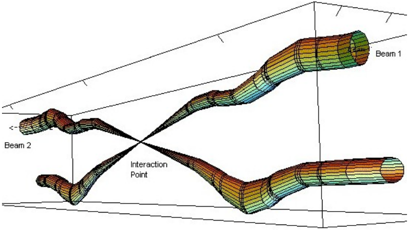

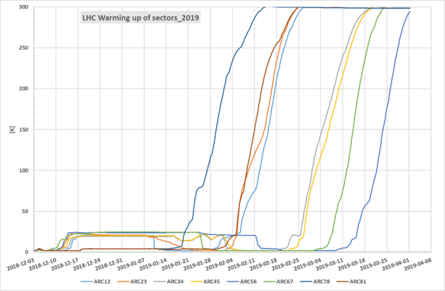

Instantaneous luminosity is a measure of how many particles are squeezed through a given space in a given time

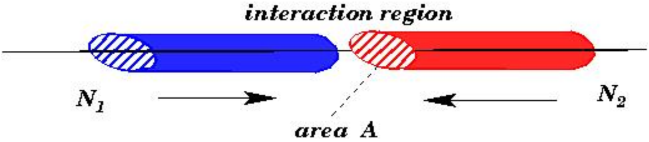

$$\mathcal{L}_{inst} = \frac{N_1 \cdot N_2 \cdot n_b \cdot f_{rev}}{A}, \quad \text{area } A = 4\pi \cdot \beta \cdot \epsilon$$

- $N_{1,2}$ - number of protons per bunch per beam 1 and 2: $\sim 1.2 \times 10^{11}$
- n_b - number of bunches: up to 2808
- f_{rev} - number of bunch turns per second: 11245
  - Proton bunches are separated by 25 ns $\rightarrow$ 40 MHz
  - Beam crossings per second: $n_b \cdot f_{rev} = 2808 * 11245 = 31575960$
  - Empty bunches for kicker magnet to dump beams
- β - amplitude function determined by interaction region focusing magnets
- ϵ - emmitance determined by quality of injected proton beams
- Peak LHC luminosity in 2018: $\mathcal{L}_{inst} = 2.2 \times 10^{34} cm^{-2} s^{-1}$ (twice the design)

- Integrated luminosity $\mathcal{L} = \int \mathcal{L}_{inst}\, dt$ is measured in inverse femtobarns:

$$\mathcal{L} = \int_{2015}^{2018} \mathcal{L}_{inst}\, dt = 158\ \text{fb}^{-1} = 158 \times 10^{39}\ \text{cm}^{-2}\ \text{(recorded with 94\% efficiency)}$$

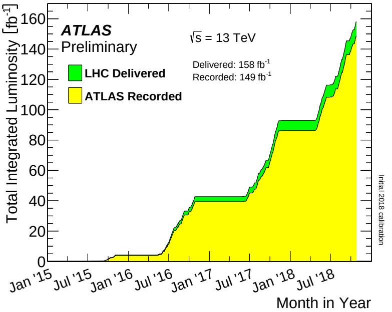

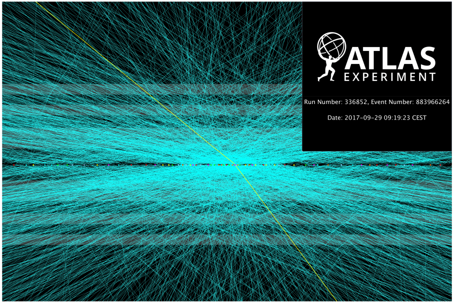

- Peak LHC luminosity of $\mathcal{L}_{inst}^{LHC} = 2.2 \times 10^{34} cm^{-2} s^{-1}$ results in:

  $\sim 32 \times 10^6$ beam crossings per second

  ~ 60 hadronic pp interactions per beam crossing

  $\sim 2 \times 10^9$ hadronic pp interactions per second

  ~ 2000 events per second recorded by the ATLAS trigger system

- Cross section is probability for two particles to interact:

$$\sigma(i \rightarrow X \rightarrow f) = \sigma_i \times \mathcal{B}_f$$

  - Narrow width approximation: resonance total width $\Gamma_X \ll$ mass M_X
  - σ_i depends on interaction type: electromagnetic, strong or weak

- Number of predicted events for a given process:

$$N_{\mathrm{predicted}}(\vec{\theta}) = \mathcal{L} \cdot \sigma_i \cdot \mathcal{B}_f \cdot A \cdot \epsilon_{exp}$$

  - $\mathcal{L}$ is integrated LHC luminosity
  - σ_i and $\mathcal{B}_f$ are predicted by the SM
  - A is detector geometrical acceptance
  - ϵ_{exp} is detector reconstruction efficiency
  - $\vec{\theta}$ encodes systematic uncertainty for the above parameters

- Maximise likelihood function to measured signal strength μ:

$$L(\mu, \vec{\theta}) = \prod_{bins} Poisson(N_{\mathrm{data}} | \mu \cdot N^{\mathrm{signal}}_{\mathrm{predicted}}(\vec{\theta}) + N^{\mathrm{background}}_{\mathrm{estimated}}(\vec{\theta}))$$

  - SM corresponds to $\mu = 1$

pp collision simulated by Sherpa event generator

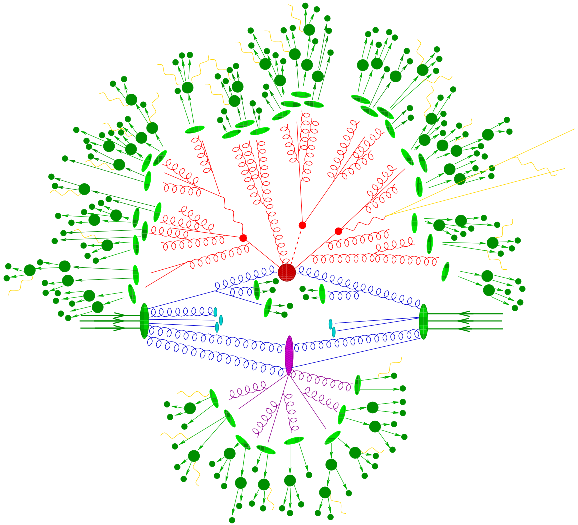

- Monte Carlo event generators to model a broad range of physics processes → produce lists of hadrons, leptons and photons
- LHC collides protons made of partons - quarks and gluons
- Typical "hard" process involves scattering of 2 partons
- Huge theory effort to model "hard" pp scattering:
  - Parton distribution functions
  - Perturbation theory
  - Hadronisation of quarks/gluons
  - Underlying event
- Next to Leading Order (NLO) in QCD for most LHC processes with MCFM, Sherpa, POWHEG, MG5_aMC@NLO, etc

Parton distribution functions (PDFs)

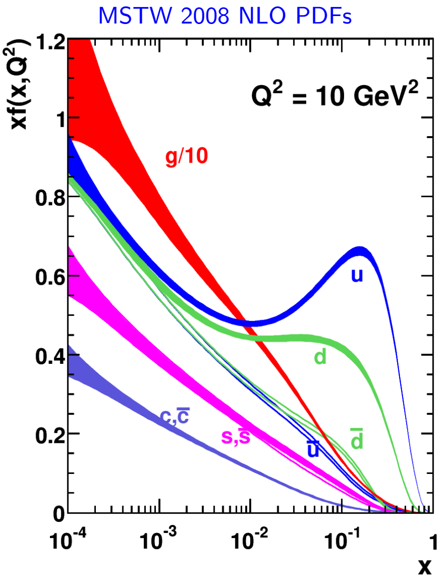

Parton distribution functions (PDFs):

- Probability for a given parton to carry momentum fraction x of the proton
- Measured from fits to collider and fixed target data
- pp cross section for final state f:

$$\sigma(pp \to f) = \sum_{a,b=q,g} \sigma(ab \to f) \otimes f_a(x_1, Q^2) \otimes f_b(x_2, Q^2)$$

- LHC collides partons with momentum distributed between 0 and 6.5 TeV
- **Longitudinal parton momenta in any given collision are unknown → only transverse momentum is conserved:** $\sum p_T = 0$
- Scattering of gluons with low x dominates LHC collisions
- Many global PDF fits: CT, MMHT,NNPDF, etc

N(experimental observables) >> N(SM parameters)

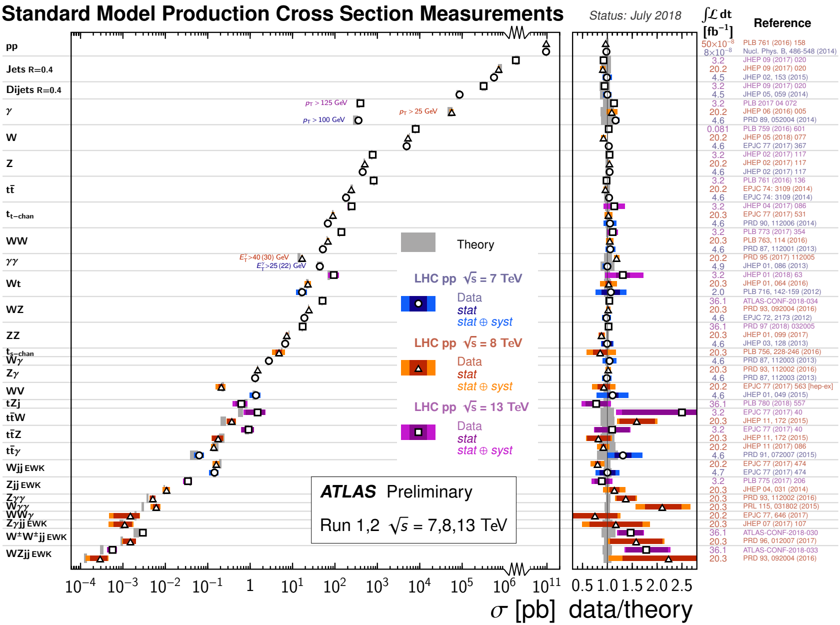

ATLAS (A Toroidal LHC ApparatuS) detector

Built and operated by more than 3000 scientists from 181 institutes in 38 countries

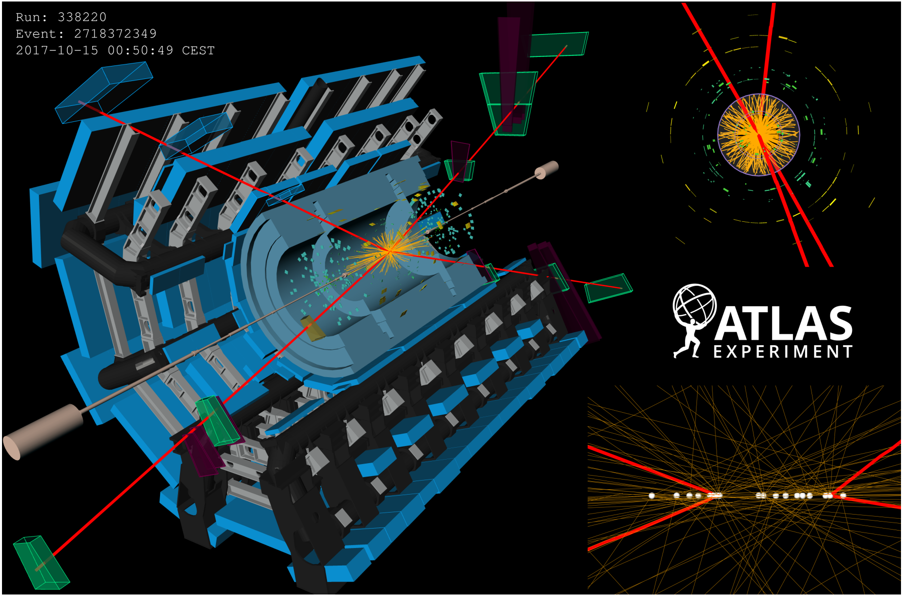

Jet reconstruction

- "Jet algorithm is set of rules... to combine particles into jets " - Gavin Salam
- Anti-k_t algorithm to reconstruct jets from calorimeter clusters - typically with $\Delta R = 0.4$

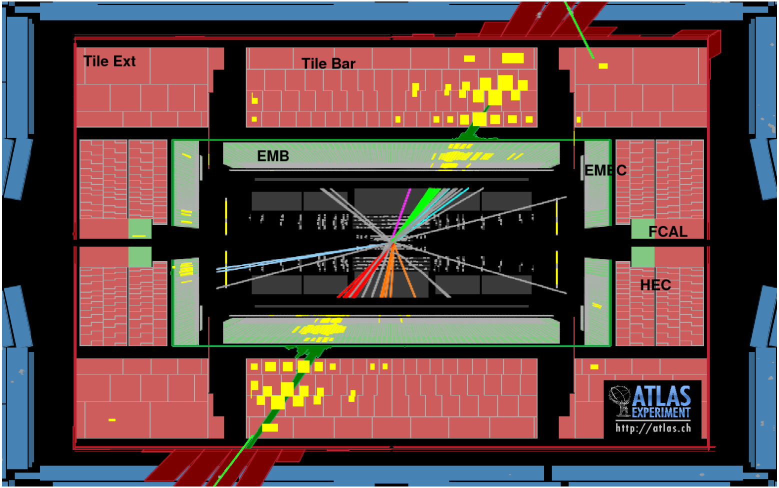

Detector geometry

- GEANT4 to simulate particle interactions with the detector material
- Rapidity is invariant under boosts along the beam axis: $y = \frac{1}{2} log \frac{E+p_z}{E-p_z}$
- Pseudorapidity is defined using azimuthal angle: $\eta = \ln \tan(\theta/2))$ - equal to y for $m = 0$
  - Tracking coverage extends to $|\eta| = 2.5$ or $\theta \approx 10^\circ$
  - Jet and electron measurements extend to $|\eta| = 4.5$ or $\theta \approx 1^\circ$
  - Angular difference is measured as $\Delta R = \sqrt{\Delta\eta^2 + \Delta\phi^2}$

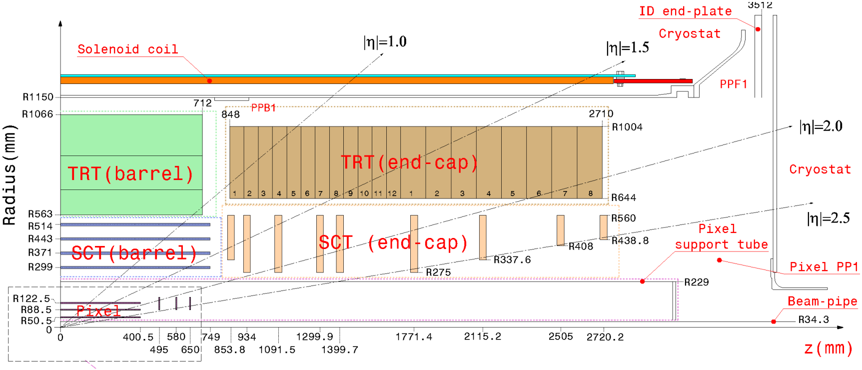

Event reconstruction

- Use calorimeter clusters and hits in the tracking detectors to reconstruct particle candidates for muons, electrons, taus and photons
  - Simulated events and data events are reconstructed using same algorithms
- Missing transverse energy: $E_T^{miss} = -\sum_{jets} E_T - \sum_{leptons} p_T - \sum_{photons} E_T - \sum_{clusters} E_T$
- Data driven calibrations rely on well understood processes: Z, J/ψ, $t\bar{t}$, etc
  - Muon and electron reconstruction efficiency is calibrated at $< 1\%$ level
  - Jet energy scale uncertainty is typically around 5%

$Z \to \mu\mu$ invariant mass

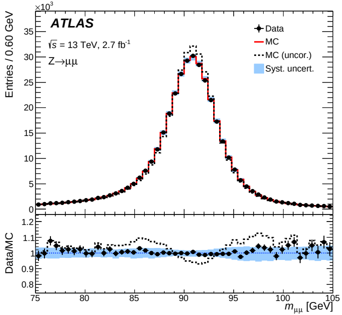

Muon reconstruction efficiency

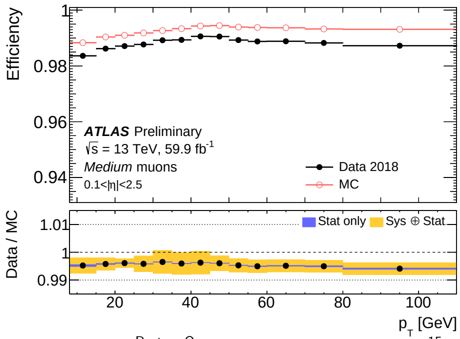

Electroweak production of same sign WW with 13 TeV data from 2015 and 2016

Electroweak production of $W^{\pm}Z$ and same sign $W^{\pm}W^{\pm}$ bosons

- Vector Boson Scattering: two quarks interact by emitting virtual W/Z bosons
- Sensitive to self-interactions of gauge bosons
- Unitarity at high energies requires presence of the SM Higgs boson

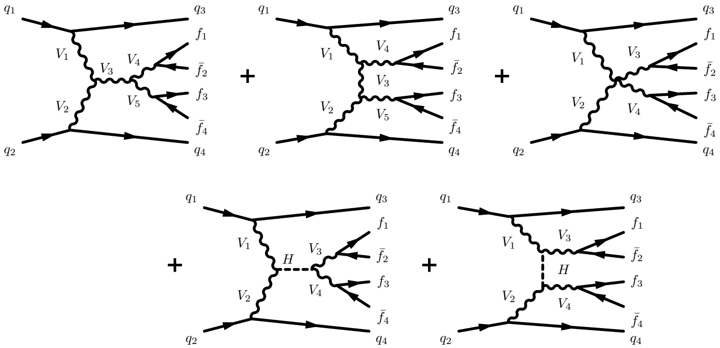

Vector Boson Scattering experimental signature:

- 2 jets with rapidity gap and large di-jet invariant mass

VVjj Vector Boson Scattering

- Example diagrams for $W^{\pm}W^{\pm}jj$ from 1708.00268
- Gauge invariance requires presence of strong production processes
- *VVjj* processes are canonically divided into two classes at Born level (Leading Order):
  - Electroweak production (EW) with weak interactions of order α_{EW}^{6}
  - Strong production (QCD) with weak and strong interactions of order $\alpha_s^2\alpha_{EW}^4$
  - Electroweak and strong interference of order $\alpha_s\alpha_{EW}^5$

EW triple coupling

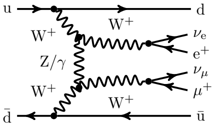

EW quartic coupling

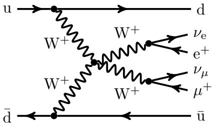

EW Higgs boson

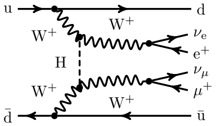

QCD

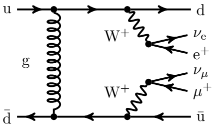

EW non-VBS

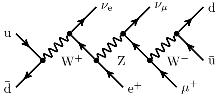

EW WWW production

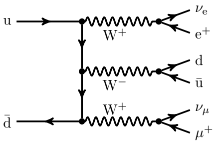

Phenomenology highlights for $W^{\pm}W^{\pm}jj$ VBS

- $W^{\pm}W^{\pm}jj$ electroweak production at LO includes couplings of order α_{EW}^{6}
  - 2 jets with rapidity gap and large invariant mass
- $W^{\pm}W^{\pm}jj$ strong production at LO includes couplings of order $\alpha_{EW}^{4}\alpha_{S}^{2}$
  - Main background process
- $W^{\pm}W^{\pm}jj$ **has the largest electroweak to strong production cross section ratio**
- *Interference between VBS and QCD processes includes couplings of order* $\alpha_{EW}^{5}\alpha_{S}$
  - Few percent contribution in the VBS signal region

Di-jet rapidity difference 1803.07943

Inclusive study at LO: $d\sigma / d|\Delta y_{j_1 j_2}|$ (fb)

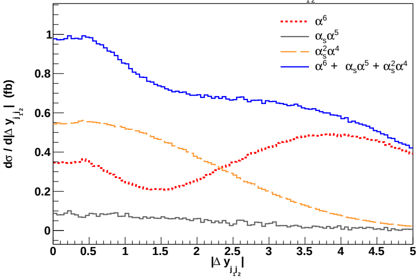

Di-jet invariant mass 1803.07943

Inclusive study at LO: $d\sigma / dm_{j_1 j_2}$ (fb/GeV)

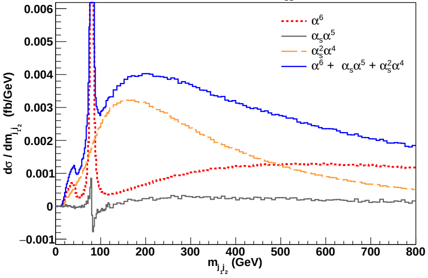

$W^{\pm}W^{\pm}jj$ experimental selection

- Isolated well reconstructed same-sign dilepton pairs: $e^{\pm}e^{\pm}$, $\mu^{\pm}\mu^{\pm}$, $e^{\pm}\mu^{\pm}$
  - Target $WW \to l\nu l\nu$ decays where l is electron or muon
  - Same sign requirement suppresses high rate SM background processes
  - Well reconstructed $\leftrightarrow$ thousands of hours of work
- Require $E_T^{miss} > 30$ GeV to tag neutrinos
- Veto third e/μ to suppress $WZ \to l^{\pm}\nu l^{+}l^{-}$ process with one lost lepton
  - Looser criteria for veto lepton for higher efficiency
- Veto b-jets to suppress $t\bar{t} \to W^{+}bW^{-}b$
  - Leptons produced in semi-leptonic B hadron decays: b-quark $\to$ jet $\to$ lepton
- Apply VBS jet selections re-optimised for 13 TeV:
  - Two leading jets with $p_T > 65, 35$ GeV
  - Dijet invariant mass $m_{jj} > 500$ GeV
  - Rapidity gap $|\Delta y_{jj}| > 2$
- Separate $++$ and $--$ channels
  - $\sigma(W^{+}W^{+}jj)/\sigma(W^{-}W^{-}jj) \sim 2.5$

$W^{\pm}W^{\pm}jj$ background processes

- WZ background is normalised from trilepton control region with 8% uncertainty
- Fake lepton background measured from control regions with 50-90% uncertainty
  - Jets mis-reconstructed as electrons
  - Electron and muons from semi-leptonic B hadron decays
  - *Dominant experimental uncertainty*
- Electron charge misidentification and $\gamma \to e$ backgrounds are measured from data
  - Electron interactions with material distort trajectory in magnetic field
- Other (irreducible) backgrounds are from Monte-Carlo simulation

Event yields before the fit

	e^+e^+	e^-e^-	$e^+\mu^+$	$e^-\mu^-$	$\mu^+\mu^+$	$\mu^-\mu^-$	combined
WZ	1.7 ± 0.6	1.2 ± 0.4	13 ± 4	8.1 ± 2.5	5.0 ± 1.6	3.3 ± 1.1	32 ± 9
Non-prompt	4.1 ± 2.4	2.3 ± 1.8	9 ± 6	6 ± 4	0.57 ± 0.16	0.67 ± 0.26	23 ± 12
e/γ conversions	1.74 ± 0.31	1.8 ± 0.4	6.1 ± 2.4	3.7 ± 1.0	-	-	13.4 ± 3.5
Other prompt	0.17 ± 0.06	0.14 ± 0.05	0.90 ± 0.24	0.60 ± 0.25	0.36 ± 0.12	0.19 ± 0.07	2.4 ± 0.5
$W^{\pm}W^{\pm}$jj strong	0.38 ± 0.13	0.16 ± 0.06	3.0 ± 1.0	1.2 ± 0.4	1.8 ± 0.6	0.76 ± 0.26	7.3 ± 2.5
Expected background	8.1 ± 2.4	5.6 ± 1.9	32 ± 7	20 ± 5	7.7 ± 1.7	4.9 ± 1.1	78 ± 15
$W^{\pm}W^{\pm}$jj electroweak	3.80 ± 0.30	1.49 ± 0.13	16.5 ± 1.2	6.5 ± 0.5	9.1 ± 0.7	3.50 ± 0.29	40.9 ± 2.9
Data	10	4	44	28	25	11	122

$W^{\pm}W^{\pm}jj$ electroweak production

Signal modelling:

- Model $W^{\pm}W^{\pm}jj$ electroweak and strong production with SHERPA 2.2.2 with up to one additional parton at LO in QCD
- NLO electroweak corrections (-16%) and interference effects ($+6\%$) are assigned as shape systematic uncertainty of m_{jj} distribution
- Alternative electroweak signal sample with POWHEG +PYTHIA8 at NLO in QCD

Likelihood fit:

- 6 channels: $e^{\pm}e^{\pm}$, $e^{\pm}\mu^{\pm}$, $\mu^{\pm}\mu^{\pm}$
- Signal region: 4 m_{jj} bins for $m_{jj} > 500 GeV$
- Control region: $200 < m_{jj} < 500 GeV$

Dijet invariant mass for $m_{jj} > 500$ GeV

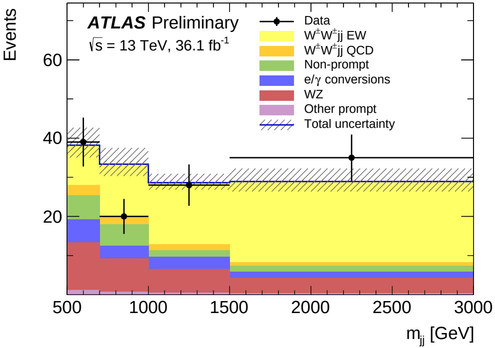

$W^\pm W^\pm jj$ electroweak production cross section

- Observed (expected with SHERPA) significance is 6.9σ (4.6σ)
- Measured fiducial cross section: $\sigma^{\rm fid}_{\rm Data} = 2.95 \pm 0.49\ ({\rm stat.}) \pm 0.23\ ({\rm sys.})\ {\rm fb}$
  - $W^\pm W^\pm jj$ strong production with exactly four EW vertices subtracted as background
  - Includes $W^\pm W^\pm jj$ electroweak production plus $\sim 4\%$ interference with strong production

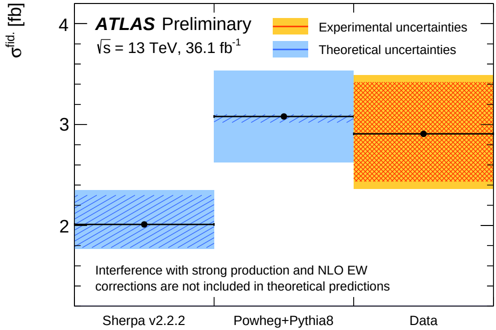

Predicted fiducial cross sections:

- POWHEG:
  $\sigma^{\rm fid}_{\rm EWK} = 3.08^{+0.45}_{-0.46}\ ({\rm syst.+stat.})\ {\rm fb}$
- SHERPA:
  $\sigma^{\rm fid}_{\rm EWK} = 2.01^{+0.33}_{-0.23}\ ({\rm sys.+stat.})\ {\rm fb}$
- SHERPA electroweak samples suffer from a non-optimal setting of colour flow for the parton shower $\rightarrow$ excess of central emissions

$W^\pm W^\pm jj$ production at NLO

- Complete QCD and electroweak NLO corrections computed for $W^\pm W^\pm jj$ 1708.00268
  - **Complete NLO correction: –17.1%**
  - Electroweak only NLO correction of order α^7_{EW}: –13.2%
  - Scale variation uncertainty is $\sim$ 2% - reduced by a factor of 5
  - Substantial LO/NLO variations for kinematic shapes

- **LHC starts to become sensitive to $W^\pm W^\pm jj$ NLO effects with full Run 2 datasets**
- Generators do not yet include EWK NLO calculations for $W^\pm W^\pm jj$
- NLO calculations are not yet available for other di-boson VBS processes

Distinctions between EW and QCD production blur at NLO

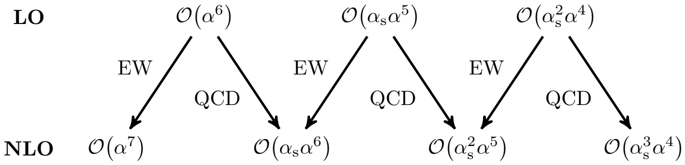

Electroweak production of WZ with 13 TeV data from 2015 and 2016

$W^{\pm}Zjj$ electroweak production

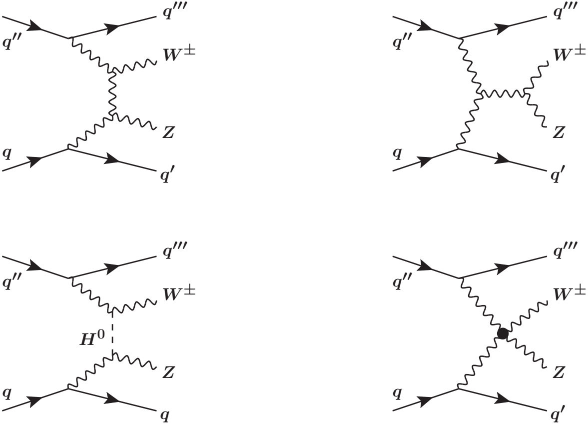

- Probe *WWZ* and *WWZZ* couplings
- Smaller electroweak production/strong production ratio compared to $W^{\pm}W^{\pm}jj$

$W^{\pm}Z$ production

Require $m_T^W > 30$ GeV

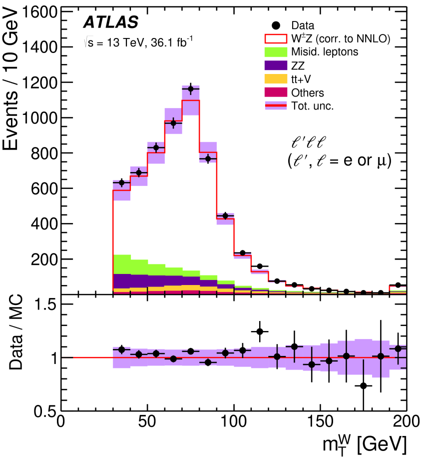

Select inclusive $W^{\pm}Z \to l^{\pm}\nu l^{+}l^{-}$ events

- 3 isolated well reconstructed electron or muon
- Veto fourth lepton to suppress $ZZ \to 4l$
- Select $Z \to e^{\pm}e^{\mp}/\mu^{\pm}\mu^{\mp}$ decays
  - $|m_{ll} - m_Z| < 10$ GeV
- Select $W^{\pm} \to e^{\pm}\nu_e/\mu^{\pm}\nu_\mu$ decays
  - Transverse mass $m_T^W > 30$ GeV
- Reconstruct jets with $p_T > 25$ GeV and $|\eta| < 4.5$

$W^{\pm}Zjj$ selections

- Next, require two or more jets with $p_T > 40$ GeV and $m_{jj} > 500$ GeV
- Boosted Decision Tree algorithm to further select EWK $W^{\pm}Zjj$ signal
  - Classification tree that learns by splitting variables into subsets
- 15 input variables describing event kinematic properties:
  - Variables computed using 2 tagging jets, W and Z bosons, jets and leptons
  - Optimised to increase sensitivity with $N - 1$ iterations
  - 3 most sensitive variables are shown below

WZ rapidity difference

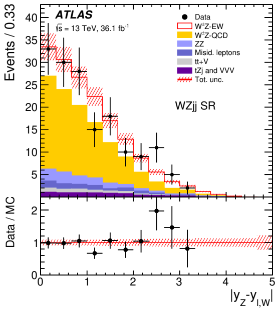

WZ centrality

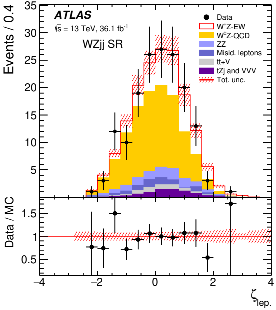

WZ transverse event balance

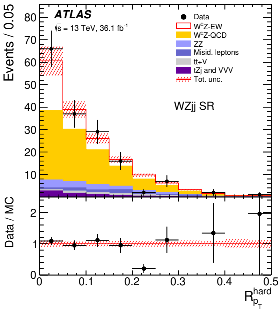

$W^{\pm}Zjj$ backgrounds

- QCD $W^{\pm}Zjj$ background is normalised from $m_{jj} < 500$ GeV control region
  - Scaled by a factor of 0.56 ± 0.16
- $t\bar{t}W$ and $t\bar{t}Z$ measured from dedicated control region
- ZZ measured from dedicated 4l control region
- Mis-reconstructed lepton background measured from data with 40% uncertainty

Event yields per region before the fit with systematic and statistical uncertainty

	SR	$WZjj$–QCD CR	b-CR	ZZ-CR
Data	161	213	141	52
Total predicted	200 ± 41	290 ± 61	160 ± 14	45.2 ± 7.5
$WZjj$–EW (signal)	24.9 ± 1.4	8.45 ± 0.37	1.36 ± 0.10	0.21 ± 0.12
$WZjj$–QCD	144 ± 41	231 ± 60	24.4 ± 1.7	1.43 ± 0.22
Misid. leptons	9.8 ± 3.9	17.7 ± 7.1	30 ± 12	0.47 ± 0.21
$ZZjj$–QCD	8.1 ± 2.2	15.0 ± 3.9	1.96 ± 0.49	35 ± 11
tZj	6.5 ± 1.2	6.6 ± 1.1	36.2 ± 5.7	0.18 ± 0.04
$t\bar{t} + V$	4.21 ± 0.76	9.11 ± 1.40	65.4 ± 10.3	2.8 ± 0.61
$ZZjj$–EW	1.80 ± 0.45	0.53 ± 0.14	0.12 ± 0.09	4.1 ± 1.4
VVV	0.59 ± 0.15	0.93 ± 0.23	0.13 ± 0.03	1.05 ± 0.30

EWK $W^{\pm}Zjj$ observation

QCD control region

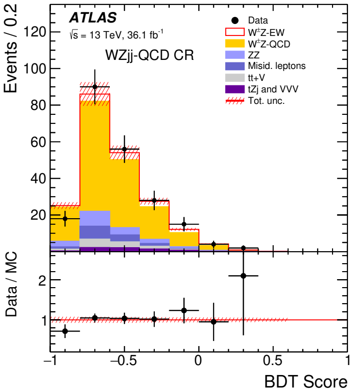

Signal region

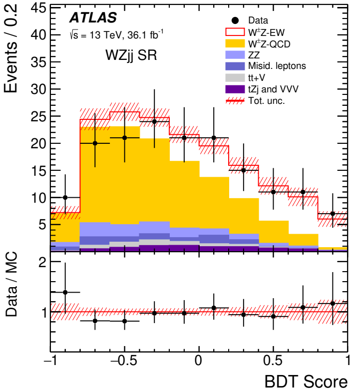

- Simultaneous fit for signal BDT template and normalisation of background processes
- Observed (expected) significance is 5.6σ (3.3σ)
- Modelling uncertainty from difference between:
  - EWK $W^{\pm}Zjj$: Sherpa2.2.2 and Madgraph LO
  - QCD $W^{\pm}Zjj$: Powheg + Herwig and Powheg + Pythia8

EWK $W^{\pm}Zjj$ observation

QCD control region

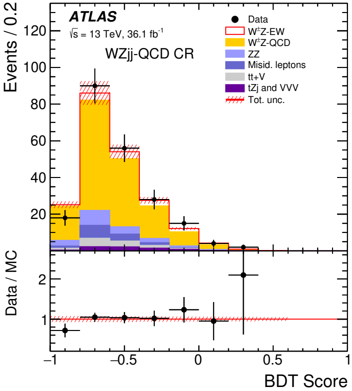

Signal region

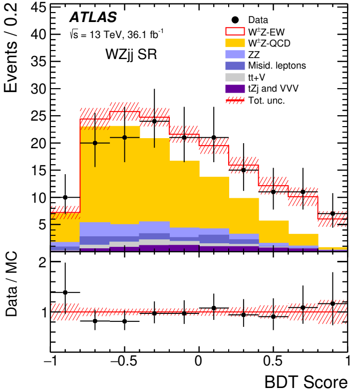

- $\sigma^{\text{fid., EW}}_{meas.} = 0.57^{+0.15}_{-0.14}$ fb (includes 10% interference contribution)

  $\sigma^{\text{fid., EW th.}}_{\text{SHERPA2.2.2}} = 0.321 \pm \text{(stat.)} \pm 0.005\ \text{(PDF)}^{+0.027}_{-0.023}\ \text{(scale) fb}$

  $\sigma^{\text{fid., EW th.}}_{\text{MADGRAPH}} = 0.366$ fb

  - Theory predictions do not include electroweak and QCD interference process
  - Similar data excess with respect to SHERPA as $W^{\pm}W^{\pm}jj$

WZ cross section with 13 TeV data from 2015 and 2016

$W^{\pm}Z$ cross section and gauge boson polarisation

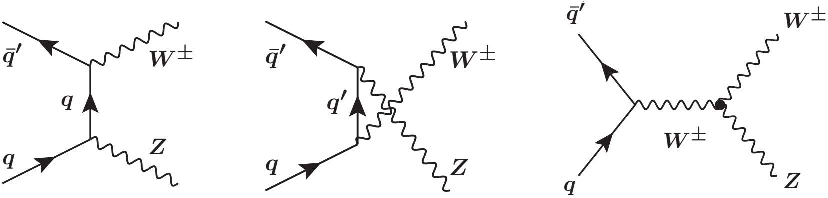

- QCD production process
- Precise measurements of differential and total cross sections
- Probe gauge structure of Standard Model
- Sensitive to anomalous triple gauge boson couplings
- Polarisation of W and Z bosons

$W^{\pm}Z$ experimental summary

Select inclusive $W^{\pm}Z \to l^{\pm}\nu l^{+}l^{-}$ events:

- 2.4% uncertainty in integrated luminosity
- Fake lepton background measured from data with 30-40% uncertainty
- e/μ efficiency mismodelling
  - 1.9% uncertainty on cross section measurement - largest detector source
- ZZ background normalised from data with 12% uncertainty
- Uncertainties for $t\bar{t}V$, tZ and VVV backgrounds vary 15% to 30%

Event yields per channel with only statistical uncertainty

Channel	eee	μee	$e\mu\mu$	$\mu\mu\mu$	All
Data	1279	1281	1671	1929	6160
Total Expected	1221 ± 7	1281 ± 6	1653 ± 8	1830 ± 7	5986 ± 14
WZ	922 ± 5	1077 ± 6	1256 ± 6	1523 ± 7	4778 ± 12
Misid. leptons	138 ± 5	34 ± 2	193 ± 5	71 ± 2	436 ± 8
ZZ	86 ± 1	89 ± 1	117 ± 1	135 ± 1	426 ± 3
$t\bar{t}$+V	50.0 ± 0.7	54 ± 0.7	56.1 ± 0.7	63.8 ± 0.8	225 ± 1
tZ	23.1 ± 0.4	24.8 ± 0.4	28.8 ± 0.4	33.5 ± 0.5	110 ± 1
VVV	2.5 ± 0.1	2.8 ± 0.1	3.2 ± 0.1	3.6 ± 0.1	12.0 ± 0.2

$W^{\pm}Z$ cross section

- Measured: $\sigma^{\text{fid.}}_{W^{\pm}Z\to\ell'\nu\ell\ell} = 63.7 \pm 1.0\,(\text{stat.}) \pm 2.3\,(\text{sys.}) \pm 0.3\,(\text{modelling}) \pm 1.5\,(\text{lumi.})$ fb.
- MATRIX: $\sigma^{\text{fid.}}_{W^{\pm}Z\to\ell'\nu\ell\ell} = 61.5^{+1.4}_{-1.3}$ fb (NNLO in QCD)
- Measured charge ratio: $\sigma^{\text{fid.}}_{W^{+}Z\to\ell'\nu\ell\ell}/\sigma^{\text{fid.}}_{W^{-}Z\to\ell'\nu\ell\ell} = 1.47 \pm 0.05\,(\text{stat.}) \pm 0.02\,(\text{sys.})$.

Precise tests of NNLO QCD calculations

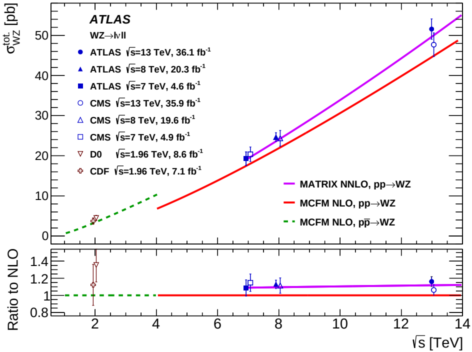

$W^{+}Z/W^{-}Z$

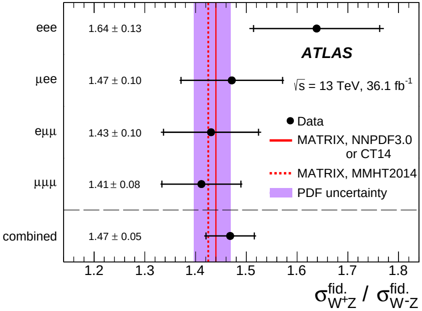

$W^{\pm}Z$ single differential cross sections

- Unfolded single differential cross sections for p_T^Z and N_{jets}, and other variables
- Response matrix obtained with POWHEG+PYTHIA8

p_T^Z

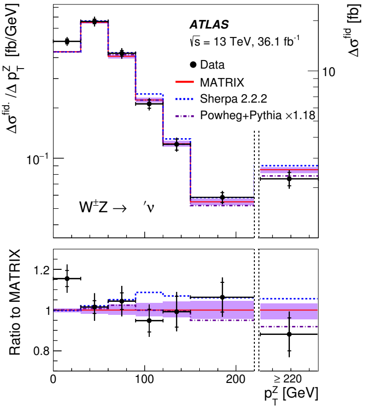

N_{jets}

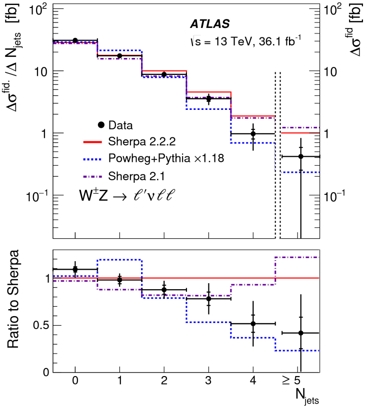

W and Z polarisation measurement

- Measure W/Z polarisation using lepton angular distributions
- f_0, f_L and f_R define the longitudinal, transverse-left handed and transverse-right handed helicity fractions at Born level (m_W constraint to solve for missing p_Z^{ν} at detector level)

$$\frac{1}{\sigma_{W^\pm Z}}\frac{d\sigma_{W^\pm Z}}{d\cos\theta_{\ell,W}} = \frac{3}{8}f_L(1\mp\cos\theta_{\ell,W})^2 + \frac{3}{8}f_R(1\pm\cos\theta_{\ell,W})^2 + \frac{3}{4}f_0\sin^2\theta_{\ell,W}$$

$l^{\pm}$ decay angle in W rest frame
with respect to WZ centre-of-mass frame

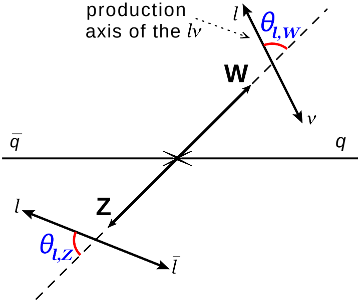

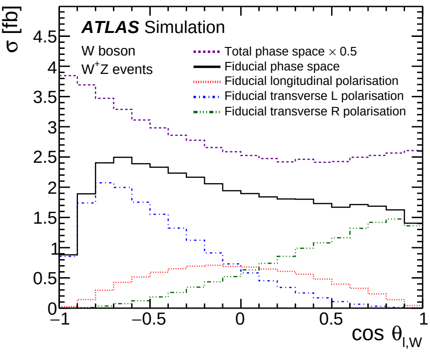

W and Z polarisation measurement

- Template fit of $q_\ell \cdot \cos\theta_{\ell,W}$ and of $\cos\theta_{\ell,Z}$ distributions
- Observed (expected) significance of 4.2σ (3.8σ) for longitudinally polarised W bosons
- Sensitive to new broad resonances not seen by direct searches

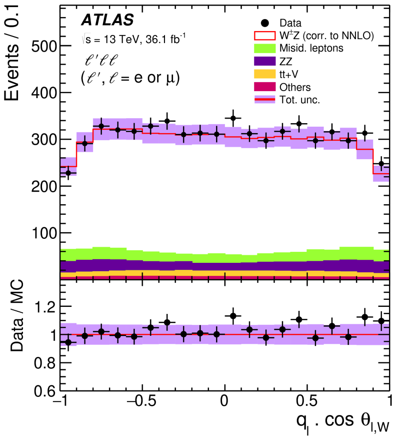

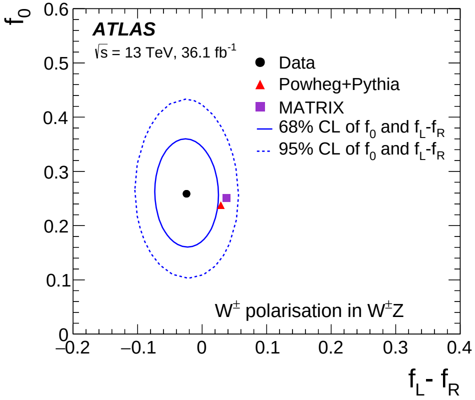

Effective leptonic weak mixing angle $\sin\theta^{l}_{\text{eff}}$ with 8 TeV data

Effective leptonic weak mixing angle

- Measure $sin^2\theta^f_{eff}$ via fermion spin correlations in $q\bar{q} \to Z/\gamma^* \to l^+l^-$ process
  - $sin^2\theta^f_{eff} = \kappa_f \times sin^2\theta_W$, where κ_f includes EW corrections
- Experiments measure **Forward-Backward** asymmetry: $A_{FB} = \frac{3}{8}A_4 = \frac{\sigma_F - \sigma_B}{\sigma_F - \sigma_B}$
  forward and backward hemispheres defined in Collins-Soper frame of the dilepton system
- At LO for given m_{ll} value: $\frac{d\sigma}{d(cos\theta^*)} \propto 1 + cos^2\theta^* + A_4 cos\theta^*$
- Different u/d quark PDF contributions and couplings to EW bosons generate A_{FB}

Strong dependence of A_{FB} on m_{ll} is due to axial and vector interference

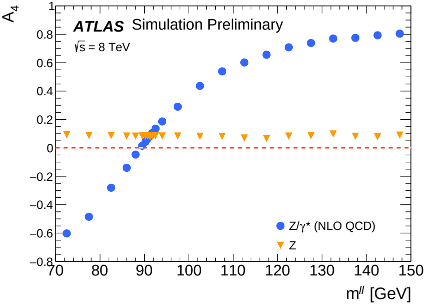

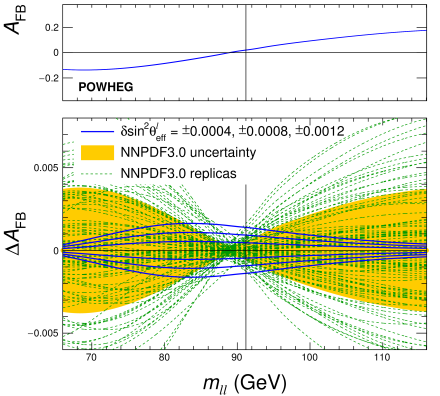

Effective leptonic mixing angle: results

- **Perform measurements using two dimensional bins of dilepton rapidity and invariant mass**
  - Fit constrains systematic uncertainty due to Parton Density Functions
  - ATLAS includes forward electrons with $2.5 < |\eta| < 4.9$ that enhance sensitivity
- PDF is dominant systematic uncertainty - comparable to statistical uncertainty
- Using $\sim$20 fb^{-1} recorded at 8 TeV - factor of $\sim$7 more data recorded at 13 TeV

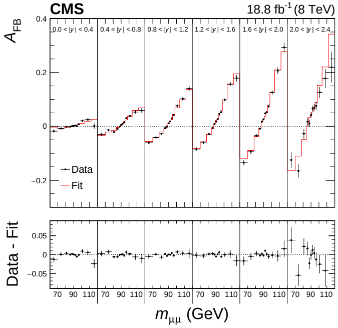

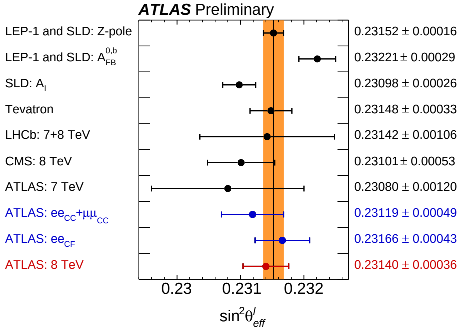

ATLAS: $\theta^{l}_{eff} = 0.23140 \pm 0.00021\ (\mathrm{stat.}) \pm 0.00024\ (\mathrm{PDF}) \pm 0.00016\ (\mathrm{syst.})$

CMS: $\theta^{l}_{eff} = 0.23101 \pm 0.00036\ (\mathrm{stat.}) \pm 0.00031\ (\mathrm{PDF}) \pm 0.00018\ (\mathrm{syst.}) \pm 0.00016\ (\mathrm{theo.})$

Summary and conclusions

- Presented recent ATLAS results probing EW sector of the SM
  - Measurements of electroweak production of same-sign WW
  - Measurements of electroweak production of WZ bosons
  - $W^{\pm}Z$ cross section and gauge boson polarisation measurements
  - Measurements of effective leptonic mixing angle
- So far, measurements agree with SM predictions up to NNLO
- These and other measurements will be improved with full Run 2 dataset
- Thank you and stay tuned for more results!

BACKUP

$W^{\pm}Zjj$ variables

- Unfolded single differential cross sections
- Response matrix obtained with POWHEG+PYTHIA8 model

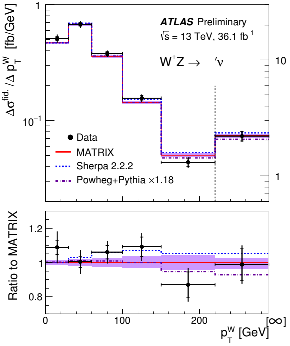

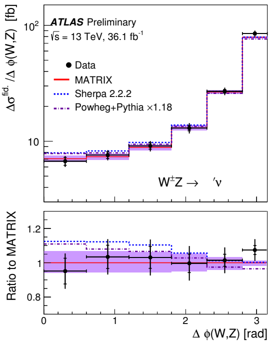

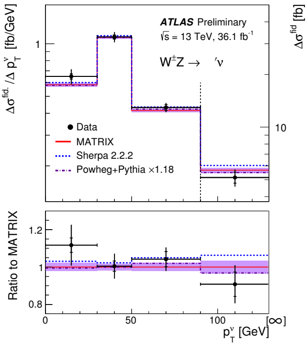

$W^{\pm}Z$ single differential cross sections

- Unfolded single differential cross sections
- Response matrix obtained with POWHEG+PYTHIA8 model

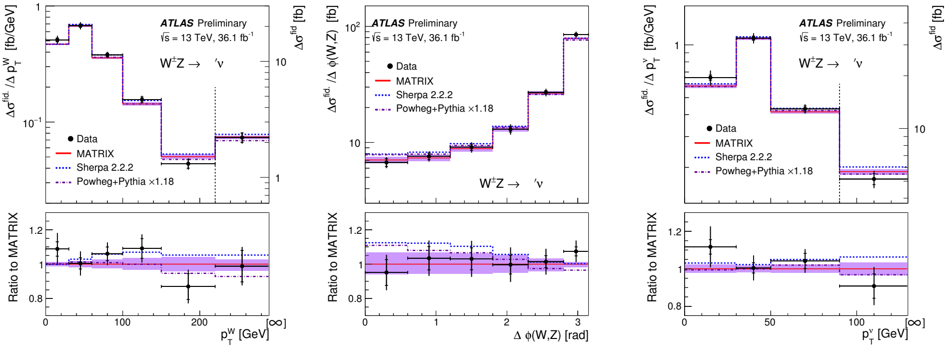

$W^{\pm}Z$ single differential cross sections

- Unfolded single differential cross sections
- Response matrix obtained with POWHEG+PYTHIA8 model

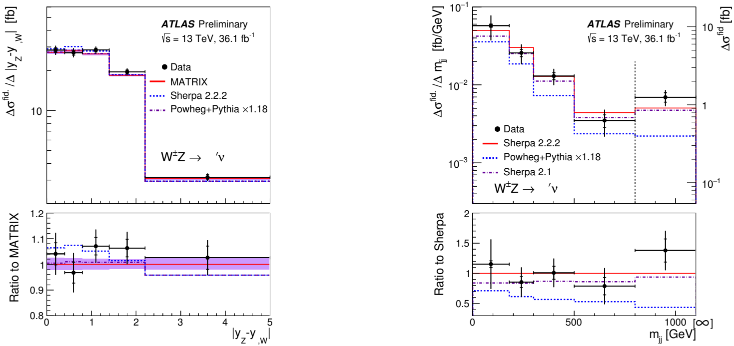

$W^{\pm}Z$ cross section

- Measured: $\sigma^{\mathrm{fid.}}_{W^{\pm}Z\to\ell'\nu\ell\ell} = 63.7 \pm 1.0\,(\mathrm{stat.}) \pm 2.3\,(\mathrm{sys.}) \pm 0.3\,(\mathrm{mod.}) \pm 1.5\,(\mathrm{lumi.})$ fb.
- MATRIX: $\sigma^{\mathrm{fid.}}_{W^{\pm}Z\to\ell'\nu\ell\ell} = 61.5^{+1.4}_{-1.3}$ fb
- $\frac{\sigma^{\mathrm{fid.}}_{W^{+}Z\to\ell'\nu\ell\ell}}{\sigma^{\mathrm{fid.}}_{W^{-}Z\to\ell'\nu\ell\ell}} = 1.47 \pm 0.05\,(\mathrm{stat.}) \pm 0.02\,(\mathrm{sys.})$.

Measured/Theory

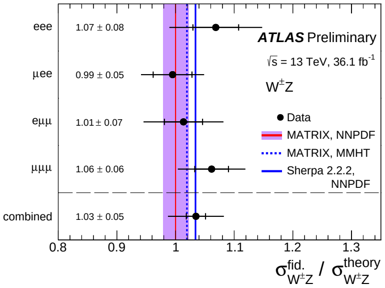

$W^{+}Z/W^{-}Z$

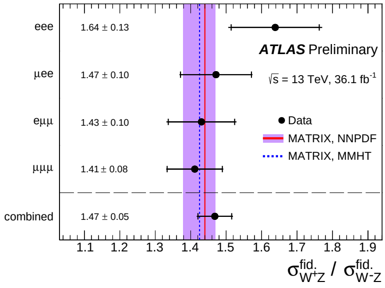

W and Z polarisation measurement

- Measure polarisation of W and Z gauge bosons using lepton angular distributions
- f_0, f_{L} and f_{R} define the longitudinal, transverse-left handed and transverse-right handed helicity fractions at Born level

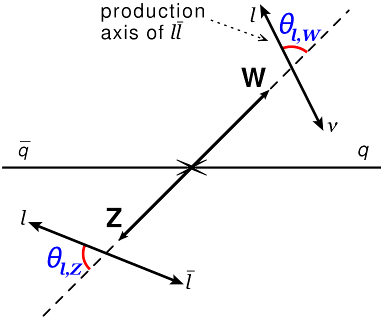

- W polarisation:
$$\frac{1}{\sigma_{W\pm Z}}\frac{d\sigma_{W\pm Z}}{d\cos\theta_{\ell,W}} = \frac{3}{8}f_{\mathrm{L}}(1\mp\cos\theta_{\ell,W})^2 + \frac{3}{8}f_{\mathrm{R}}(1\pm\cos\theta_{\ell,W})^2 + \frac{3}{4}f_0\sin^2\theta_{\ell,W}$$
- Z polarisation:
$$\frac{1}{\sigma_{W\pm Z}}\frac{d\sigma_{W\pm Z}}{d\cos\theta_{\ell,Z}} = \frac{3}{8}f_{\mathrm{L}}(1+2\alpha\cos\theta_{\ell,Z}+\cos^2\theta_{\ell,Z}) + \frac{3}{8}f_{\mathrm{R}}(1+\cos^2\theta_{\ell,Z}-2\alpha\cos\theta_{\ell,Z}) + \frac{3}{4}f_0\sin^2\theta_{\ell,Z}$$

Observation of $W^{\pm}W^{\pm}jj$ electroweak production

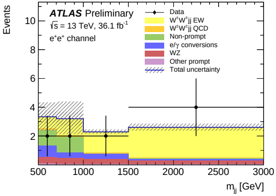

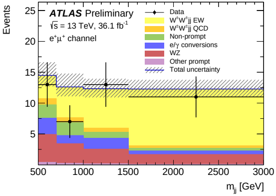

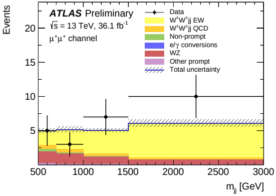

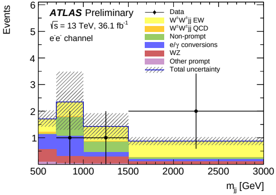

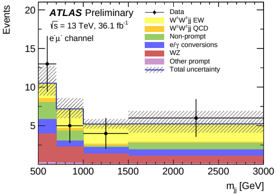

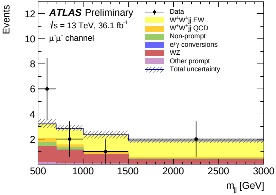

Observation of $W^{\pm}W^{\pm}jj$ electroweak production

- Both experiments reported observation of $W^{\pm}W^{\pm}jj$ electroweak production
  - Enhancement of data events at high m_{jj} values - classical VBS signature
  - Measurement uncertainty is dominated by statistical data uncertainty
  - Mis-identified leptons are important experimental background

Observed significance 5.5σ

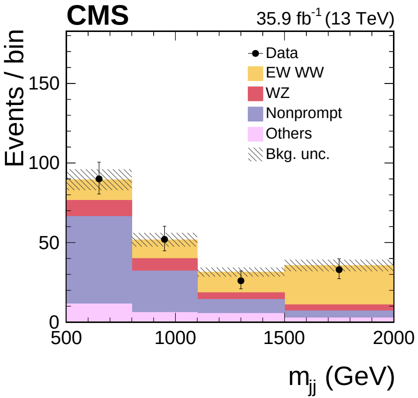

Observed significance 6.9σ

Presented yesterday by Liqing Zhang

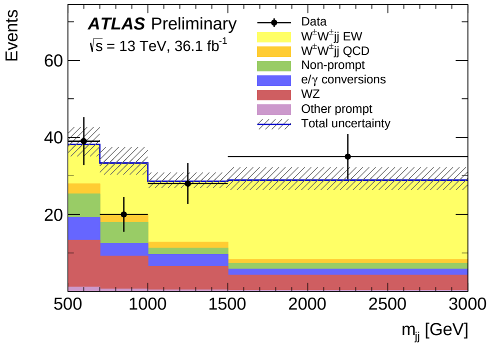

Measurements of $W^{\pm}Zjj$ electroweak production

- CMS performs 2d fit using m_{jj} and $\Delta\eta_{jj}$ variables
  - $W^{\pm}Zjj$ QCD background process normalised from data: $\mu^{QCD}_{W^{\pm}Zjj} \sim 1$
- ATLAS performs multi-variate analysis - 15 kinematic variables to select $W^{\pm}Zjj$ VBS signal
  - $W^{\pm}Zjj$ QCD background process normalised from data: $\mu^{QCD}_{W^{\pm}Zjj} = 0.60 \pm 0.25$

Obs. (exp.) significance 1.9σ (2.7σ)

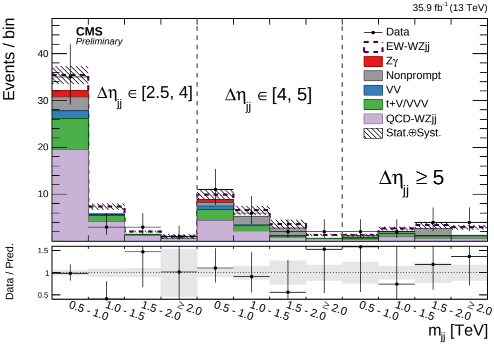

Obs. (exp.) significance 5.6σ (3.3σ)

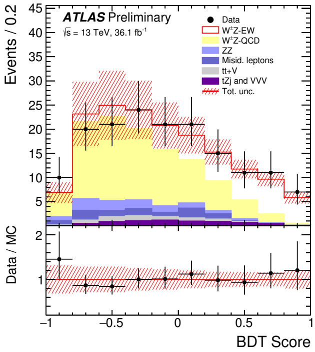

$W^{\pm}Z$ cross section and gauge boson polarisation

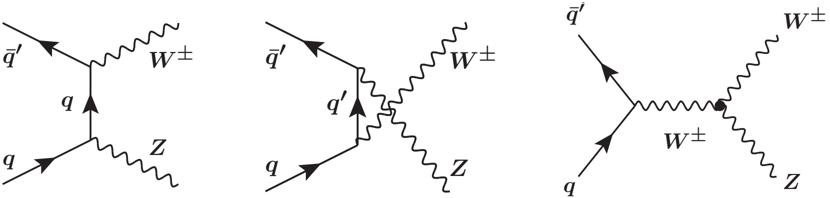

- Probe gauge structure of Standard Model
- Sensitive to anomalous triple gauge boson couplings
- Precise measurements of differential and total cross sections
- Polarisation of W and Z bosons

$W^{\pm}Z$ production

Trilepton fiducial region:

- Select $Z \to e^{\pm}e^{\mp}/\mu^{\pm}\mu^{\mp}$ decays
  - $p_T^{e,\mu} > 15$ GeV and $|\eta^{e,\mu}| < 2.5$
  - $|m_{ll} - m_Z| < 10$ GeV
- Select $W^{\pm} \to e^{\pm}\nu_e/\mu^{\pm}\nu_\mu$ decays
  - $p_T^{e,\mu} > 15$ GeV and $|\eta^{e,\mu}| < 2.5$
  - Transverse mass $m_T^W > 30$ GeV
- Anti-kt 0.4 jets with $p_T > 25$ GeV and $|\eta| < 4.5$

Signal modelling:

- Model $W^{\pm}Z$ with POWHEG at NLO in QCD
- Shower with PYTHIA8 8.210 and CTEQ6L1PDF
- Shower with HERWIG to estimate uncertainty

Theory predictions:

- NNLO QCD $W^{\pm}Z$ cross sections with MATRIX
  - Apply particle-to-parton level corrections

Require $m_T^W > 30$ GeV

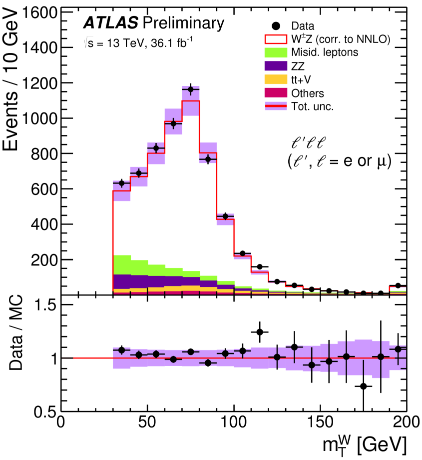

$W^{\pm}Z$ experimental summary

Experimental selections:

- 3 isolated well reconstructed e and μ, veto fourth lepton to suppress ZZ
- Separate and combined measurements for 4 lepton flavour channels

Backgrounds and experimental uncertainty:

- Fake lepton background measured from data with 30-40% uncertainty
  - 1.9% uncertainty on cross section measurement
- ZZ background normalised from data with 12% uncertainty
- Uncertainties for $t\bar{t}V$, tZ and VVV backgrounds vary 15% to 30%
- e/μ efficiency mismodelling - up to 1.5% uncertainty on cross section measurement
- Integrated luminosity - 2.4% uncertainty on cross section measurement

Event yields per channel with only statistical uncertainty

Channel	eee	μee	$e\mu\mu$	$\mu\mu\mu$	All
Data	1279	1281	1671	1929	6160
Total Expected	1221 ± 7	1281 ± 6	1653 ± 8	1830 ± 7	5986 ± 14
WZ	922 ± 5	1077 ± 6	1256 ± 6	1523 ± 7	4778 ± 12
Misid. leptons	138 ± 5	34 ± 2	193 ± 5	71 ± 2	436 ± 8
ZZ	86 ± 1	89 ± 1	117 ± 1	135 ± 1	426 ± 3
$t\bar{t}$+V	50.0 ± 0.7	54 ± 0.7	56.1 ± 0.7	63.8 ± 0.8	225 ± 1
tZ	23.1 ± 0.4	24.8 ± 0.4	28.8 ± 0.4	33.5 ± 0.5	110 ± 1
VVV	2.5 ± 0.1	2.8 ± 0.1	3.2 ± 0.1	3.6 ± 0.1	12.0 ± 0.2

$W^{\pm}Z$ cross section

- Measured: $\sigma^{\text{fid.}}_{W^{\pm}Z\to\ell'\nu\ell\ell} = 63.7 \pm 1.0\,(\text{stat.}) \pm 2.3\,(\text{sys.}) \pm 0.3\,(\text{modelling}) \pm 1.5\,(\text{lumi.})$ fb.
- MATRIX: $\sigma^{\text{fid.}}_{W^{\pm}Z\to\ell'\nu\ell\ell} = 61.5^{+1.4}_{-1.3}$ fb
- Measured charge ratio: $\sigma^{\text{fid.}}_{W^{+}Z\to\ell'\nu\ell\ell}/\sigma^{\text{fid.}}_{W^{-}Z\to\ell'\nu\ell\ell} = 1.47 \pm 0.05\,(\text{stat.}) \pm 0.02\,(\text{sys.})$.

Precise tests of NNLO QCD calculations

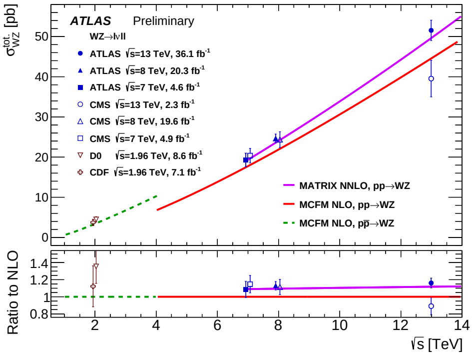

$W^{+}Z/W^{-}Z$

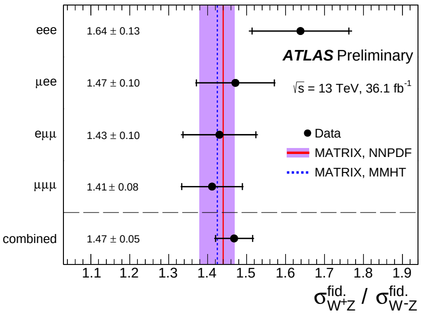

$W^{\pm}Z$ single differential cross sections

- Unfolded single differential cross sections for p_T^Z, M_T^{WZ}, N_{jets} (below) and other variables
- Response matrix obtained with POWHEG+PYTHIA8

p_T^Z

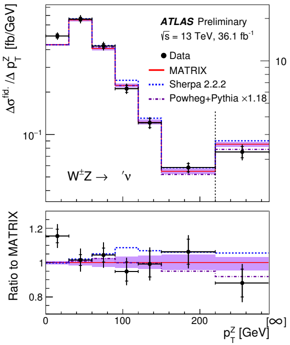

M_T^{WZ}

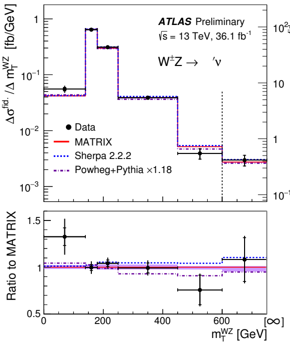

N_{jets}

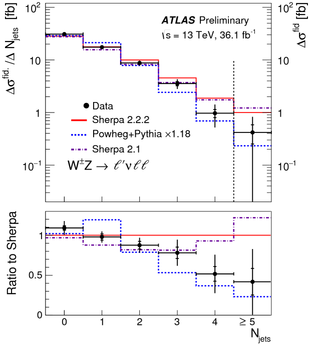

W and Z polarisation measurement

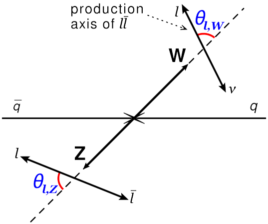

- Measure W/Z polarisation using lepton angular distributions
- f_0, f_L and f_R define the longitudinal, transverse-left handed and transverse-right handed helicity fractions at Born level
- Template fit of $q_\ell \cdot \cos\theta_{\ell,W}$ and of $\cos\theta_{\ell,Z}$ distributions
  - m_W constraint to solve for missing p_Z^ν at detector level

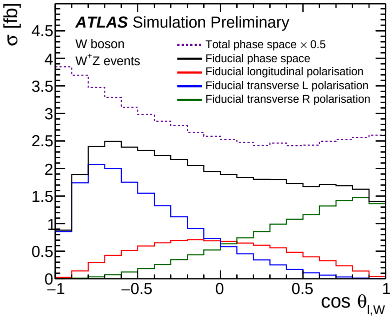

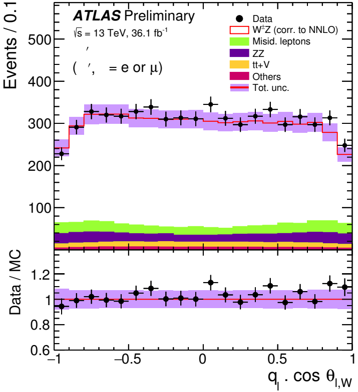

W and Z polarisation measurement

- Observed (expected) significance of 4.2σ (3.8σ) for longitudinally polarised W bosons
- Sensitive to new broad resonances not seen by direct searches

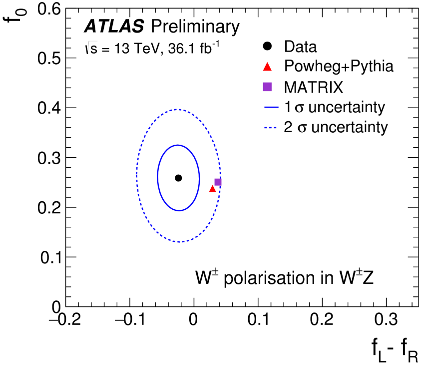

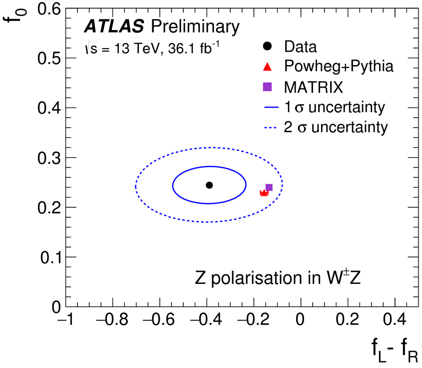

Charged gauge boson self-couplings are present at tree level in SM:

- Quartic couplings: $WWZZ$, $WWWW$, $WWZ\gamma$, $WW\gamma\gamma$
- Triple couplings: WWZ, $WW\gamma$

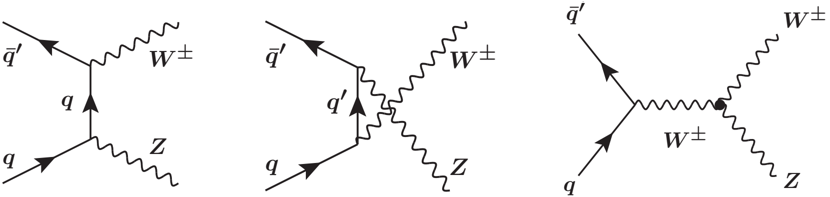

$W^\pm Z$ cross section and gauge boson polarisation

- Sensitive to anomalous triple gauge boson couplings
- Select leptonic decays for clean experimental detection: $W^\pm Z \to l^\pm \nu l^+ l^-$

$W^{\pm}Z$ cross section

- $W^{\pm}Z$ total cross section measured by CMS:
  - Measured: $\sigma_{W^{\pm}Z} = 48.09^{+1.00}_{-0.96}\,(\mathrm{stat})^{+0.44}_{-0.37}\,(\mathrm{theo})^{+2.39}_{-2.17}\,(\mathrm{syst}) \pm 1.39(\mathrm{lumi})$ pb
  - MATRIX: $\sigma_{W^{\pm}Z} = 49.98^{+1.1}_{-1.0}$ pb (NNLO in perturbative QCD)
- Also measure precise fiducial and differential cross sections
- Experimental uncertainty is reduced for $W^{+}Z/W^{-}Z$ ratio - comparable to NNLO accuracy

Differential p_Z cross section
CMS-PAS-SMP-18-002

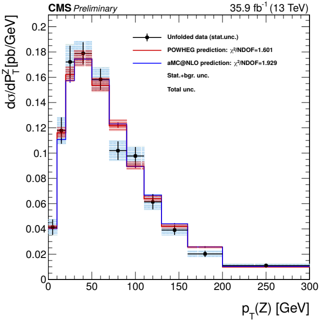

Measure $W^{+}Z/W^{-}Z$ ratio
ATLAS-CONF-2018-034

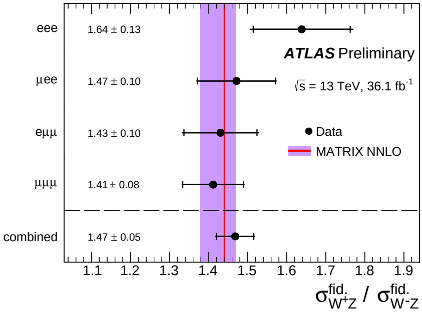

$W^{\pm}Z$: limits on anomalous couplings

- CMS set limits on anomalous couplings using Effective Field Theory approach:
  $\delta\mathcal{L}_{\mathrm{AC}} = c_{WWW} \times Tr[W_{\mu\nu}W^{\nu\rho}W^{\mu}_{\rho}] + c_W \times (D_\mu H)^\dagger W^{\mu\nu}(D_\nu H) + c_b \times (D_\mu H)^\dagger B^{\mu\nu}(D_\nu H)$
- Test m_{WZ} distribution for deviations from SM predictions

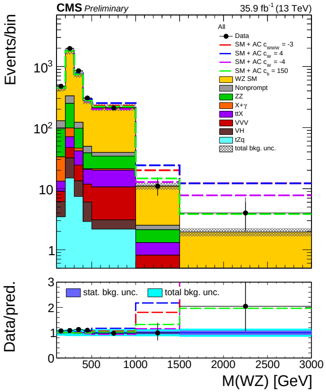

Anomalous coupling limits

[CMS-PAS-SMP-18-002]

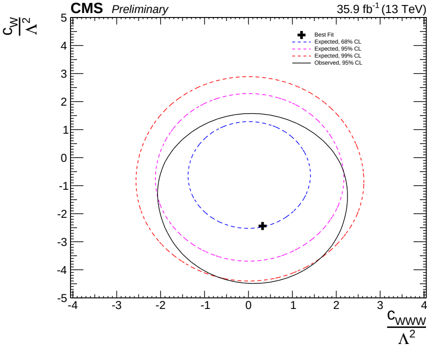

W and Z polarisation measurement

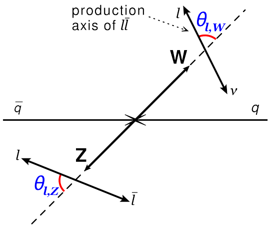

- Measure W/Z polarisation using lepton angular distributions
- f_0, $f_{\rm L}$ and $f_{\rm R}$ define the longitudinal, transverse-left handed and transverse-right handed helicity fractions at Born level
- Observed (expected) significance of 4.2σ (3.8σ) for longitudinally polarised W bosons
- Sensitive to new broad resonances not seen by direct searches

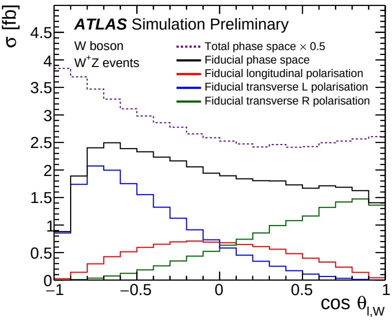

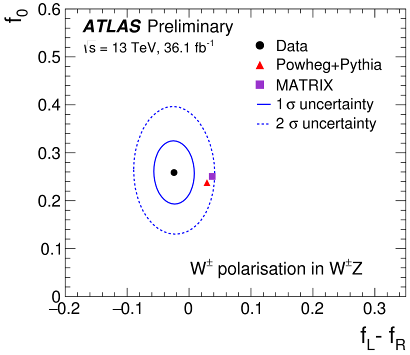

Electroweak production of same-sign *WW* and *WZ* bosons

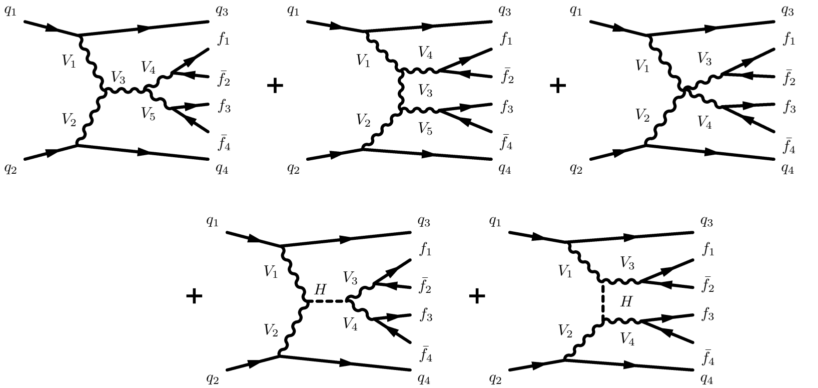

- Measure self-interactions of heavy gauge bosons
- Unitarity at high energies requires presence of the SM Higgs boson

$W^{\pm}W^{\pm}jj$ electroweak production

Same-sign dilepton fiducial region:

- Same-sign dilepton events with $m_{ll} > 20$ GeV
  - e or μ with $p_T > 27$ GeV and $|\eta| < 2.5$
- Neutrinos with $p_T^{\nu\nu} > 30$ GeV
- Anti-kit 0.4 jets with $|\eta| < 4.5$
- Optimised VBS jet selections:
  - Two leading jets with $p_T > 65, 35$ GeV
  - Dijet invariant mass $m_{jj} > 500$ GeV
  - Rapidity gap $|\Delta y_{jj}| > 2$

Signal modelling:

- Model $W^{\pm}W^{\pm}jj$ electroweak and strong production with SHERPA 2.2.2
- Alternative NLO in QCD sample with with POWHEG +PYTHIA88 for electroweak signal
- $W^{\pm}W^{\pm}jj$ strong production with exactly four EW vertices subtracted as background

Dijet invariant mass for $m_{jj} > 500$ GeV

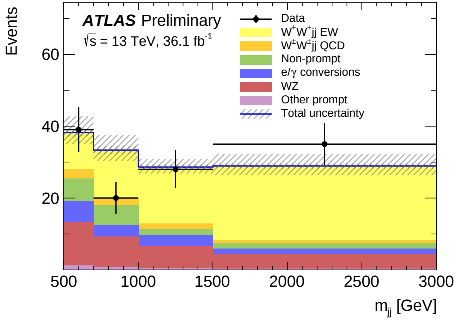

Likelihood fit:

- 6 channels: $e^{\pm}e^{\pm}$, $e^{\pm}\mu^{\pm}$, $\mu^{\pm}\mu^{\pm}$
- Signal region: 4 m_{jj} bins for $m_{jj} > 500 GeV$
- Control region: $200 < m_{jj} < 500 GeV$

$W^{\pm}W^{\pm}jj$ experimental summary

Experimental selection:

- Isolated well reconstructed same-sign dilepton events (e or μ)
- Veto third lepton to suppress WZ and veto b-jets to suppress $t\bar{t}$
- Require $E_T^{miss} > 30$ GeV and VBS jet selections

Backgrounds and experimental uncertainty:

- WZ background is normalised from trilepton control region with 8% uncertainty
- Fake lepton background measured from control regions with 50-90% uncertainty
  - Dominant experimental uncertainty
- Electron charge misidentification and $\gamma \to e$ backgrounds are measured from data
- Other irreducible backgrounds are from Monte-Carlo simulation

Event yields before the fit

	e^+e^+	e^-e^-	$e^+\mu^+$	$e^-\mu^-$	$\mu^+\mu^+$	$\mu^-\mu^-$	combined
WZ	1.7 ± 0.6	1.2 ± 0.4	13 ± 4	8.1 ± 2.5	5.0 ± 1.6	3.3 ± 1.1	32 ± 9
Non-prompt	4.1 ± 2.4	2.3 ± 1.8	9 ± 6	6 ± 4	0.57 ± 0.16	0.67 ± 0.26	23 ± 12
e/γ conversions	1.74 ± 0.31	1.8 ± 0.4	6.1 ± 2.4	3.7 ± 1.0	-	-	13.4 ± 3.5
Other prompt	0.17 ± 0.06	0.14 ± 0.05	0.90 ± 0.24	0.60 ± 0.25	0.36 ± 0.12	0.19 ± 0.07	2.4 ± 0.5
$W^{\pm}W^{\pm}$jj strong	0.38 ± 0.13	0.16 ± 0.06	3.0 ± 1.0	1.2 ± 0.4	1.8 ± 0.6	0.76 ± 0.26	7.3 ± 2.5
Expected background	8.1 ± 2.4	5.6 ± 1.9	32 ± 7	20 ± 5	7.7 ± 1.7	4.9 ± 1.1	78 ± 15
$W^{\pm}W^{\pm}$jj electroweak	3.80 ± 0.30	1.49 ± 0.13	16.5 ± 1.2	6.5 ± 0.5	9.1 ± 0.7	3.50 ± 0.29	40.9 ± 2.9
Data	10	4	44	28	25	11	122

$W^{\pm}W^{\pm}jj$ electroweak production cross section

- Observed (expected with SHERPA) significance is 6.9σ (4.6σ)
- Measured fiducial cross section: $\sigma^{\rm fid}_{\rm Data} = 2.95 \pm 0.49\,({\rm stat.}) \pm 0.23\,({\rm sys.})$ fb
  - $\sigma^{\rm fid}_{\rm Data}$ includes $W^{\pm}W^{\pm}jj$ electroweak plus interference with $W^{\pm}W^{\pm}jj$ strong
  - $W^{\pm}W^{\pm}jj$ strong production with exactly four EW vertices subtracted as background

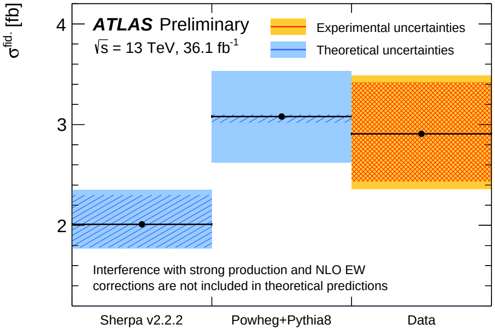

Predicted fiducial cross sections:

- POWHEG: $\sigma^{\rm fid}_{\rm EWK} = 3.08^{+0.45}_{-0.46}$ (syst.+stat.) fb
- SHERPA: $\sigma^{\rm fid}_{\rm EWK} = 2.01^{+0.33}_{-0.23}$ (sys.+stat.) fb
- NLO electroweak corrections (-16% for SHERPA) and interference ($+6\%$) are not included